Connectivity between seamounts and coastal ecosystems in the Southwestern Indian Ocean

Estelle Crochelet, Nicolas Barrier, Marco Andrello, Francis Marsac, Aurélie Spadone, Christophe Lett

Connectivity between seamounts and coastal ecosystems in the Southwestern Indian Ocean

Crochelet Estelle [1, 2, *], Barrier Nicolas [3, 4], Andrello Marco [3, 4], Marsac Francis [3, 4], Spadone Aurélie [5], Lett Christophe [3, 4]

[1] ARBRE - Agence de Recherche pour la Biodiversité à la Réunion, 34 avenue de la Grande Ourse, 97434, Saint-Gilles, La Réunion, France
[2] IRD / ESPACE-DEV (UMR 228), Parc Technologique Universitaire, 2 rue Joseph Wetzell, CS 41 095, 97495, Sainte Clotilde Cedex, La Réunion, France
[3] Institut de Recherche pour le Développement (IRD), Sète, France
[4] MARBEC, Univ Montpellier, CNRS, Ifremer, IRD, Sète, France
[5] IUCN – International Union for Conservation of Nature, Gland, Switzerland

* Corresponding author : Etelle Crochelet, email address : estelle.crochelet@ird.fr

nicolas.barrier@ird.fr ; marco.andrello@gmail.com ; francis.marsac@ird.fr ; aurelie.spadone@iucn.org ; christophe.lett@ird.fr

Abstract :

Understanding larval connectivity patterns is critical for marine spatial planning, particularly for designing marine protected areas and managing fisheries. Patterns of larval dispersal and connectivity can be inferred from numerical transport models at large spatial and temporal scales. We assess model-based connectivity patterns between seamounts of the Southwestern Indian Ocean (SWIO) and the coastal ecosystems of Mauritius, La Réunion, Madagascar, Mozambique and South Africa, with emphasis on three shallow seamounts (La Pérouse [LP], MAD-Ridge [MR] and Walters Shoal [WS]). Using drifter trajectory and a Lagrangian model of ichthyoplankton dispersal, we show that larvae can undertake very long dispersion, with larval distances increasing with pelagic larval duration (PLD). There are three groups of greater connectivity: the region between the eastern coast of Madagascar, Mauritius and La Réunion islands; the seamounts of the South West Indian Ridge; and the pair formed by WS and a nearby un-named seamount. Connectivity between these three groups is evident only for the longest PLD examined (360 d). Connectivity from seamounts to coastal ecosystems is weak, with a maximum of 2% of larvae originating from seamounts reaching coastal ecosystems. Local retention at the three focal seamounts (LP, MR and WS) peaks at about 11% for the shortest PLD considered (15 d) at the most retentive seamount (WS) and decreases sharply with increasing PLD. Information on PLD and age of larvae collected at MR and LP are used to assess their putative origin. These larvae are likely self-recruits but it is also plausible that they immigrate from nearby coastal sites, i.e. the southern coast of Madagascar for MR and the islands of La Réunion and Mauritius for LP.

Keywords : Seamounts, connectivity, larval duration, larval drift, Lagrangian modelling, biophysical model, surface drifters, Southwestern Indian Ocean, Ichthyop.

1. Introduction

Marine resources are under threat from the combined effects of climate change, overfishing, pollution, diseases, tourism and coastal development (FAO, 2018). As marine ecosystems degrade, so do the well-being and livelihoods of populations that depend directly on the ecosystem goods and services they provide (Moberg and Folke, 1999). Managing marine resources effectively is therefore crucial, from both social and ecological perspectives. Connectivity is recognized as a key factor affecting marine populations dynamics, population persistence and stock sustainability (Hastings and Botsford, 2006), as well as the efficiency of management strategies in the face of global changes. It is defined as "the exchange of individuals among geographically separated subpopulations" (Cowen et al., 2007). Transport processes are believed to connect distant populations. Despite early genetic studies showing a fair degree of homogeneity between populations over large spatial scales (Doherty et al., 1995), accumulating recent evidence suggests that populations are not as open as initially thought. High levels of local retention and low levels of long-distance dispersal could be maintained by mesoscale and sub-mesoscale eddies capable of transporting larvae back to their location of origin despite long pelagic larval durations (Cowen et al., 2000; Warner and Cowen, 2002), thereby contributing to maintain endemic species around isolated islands (Boehlert et al., 1992).

The majority of marine organisms have a bipartite life history and experience pelagic larval stages before they settle and become sedentary (Leis, 1991). Larvae remain in the midwater layers for days to months while they acquire swimming and sensory capabilities that enable them to control part of their dispersal (Kingsford *et al.*, 2002; Leis, 2002). This pelagic stage facilitates the transport of individuals among spatially isolated populations. It has been suggested that the pelagic larval duration (PLD) is the most important factor determining the

76 level of larval dispersal and connectivity (Riginos and Victor, 2001; Selkoe and Toonen,

77 2011; Luiz et al., 2013). Connectivity between distant populations may indeed be favoured by

78 long PLD, whereas larval settlement close to the natal habitat can result from short PLD and

79 entail increased population differentiation over short scales (Planes et al., 2001). However,

80 larval dispersal is also mediated by both complex and dynamic oceanographic features and

81 biological properties (Pineda et al., 2009).

82

83 The effective management of marine resources requires estimating the realized levels of

84 connectivity between populations, but empirical estimates are scarce (Manel et al., 2019).

85 Indeed, marine larvae are notoriously difficult to monitor, due to their small size and possibly

86 long dispersal distances, up to hundreds of kilometers from their initial release site (Leis,

87 1984; Victor, 1987). Patterns of larval dispersal and connectivity also vary between species.

88 Various methods such as population genetics and phylogeography, microchemical

89 fingerprinting, stable isotopes, otolith microchemistry, otolith shape analysis and biophysical

90 dispersal models have been developed to assess patterns of larvae dispersal and population

91 connectivity across the marine environment (Schultz and Cowen, 1994; Roberts, 1997;

92 Cowen et al., 2000; Hellberg, 2007; Treml et al., 2008; Jones et al., 2009; Mora et al., 2012,

93 Bryan-Brown et al., 2018).

94

95 The South West Indian Ocean (SWIO) has a high level of marine biodiversity, and marine

96 species in the region are widely used as food resources and provide economic benefits to a

97 rapidly growing human population. However, the SWIO is one of the less studied regions of

98 the world (Obura, 2012; UNEP-Nairobi Convention and WIOMSA, 2015).

99

100 The SWIO has many seamounts. Seamount ecosystems are recognized as critical habitats for

101 a wide array of species (Clark et al., 2012) and are subject to anthropogenic exploitation

102 (Rowden et al., 2010). Despite an increased focus on these particular ecosystems, the natural

103 processes involved to sustain biodiversity at seamounts remain largely unknown, in particular

104 in the SWIO. Seamounts are generally geographically isolated structures, but currents can

105 ensure connectivity between them and with adjacent ecosystems.

106

107 In this paper, we consider nine seamounts of the SWIO, ranging from latitudes 15°S to 45°S

108 (Figure 1), which were the focus of previous oceanographic campaigns (Southern Indian

109 Ocean Seamounts Project in 2009: Read and Pollard, 2017; Rogers et al., 2017; Pollard and

110 Read, 2017). Five of them belong to the South West Indian Ridge (SWIR, 25–50°S), an area

111 delineated by elevated rims reaching up to 2000 m below sea level, with several seamounts on

112 its flanks rising to only a few hundred metres below the surface (Guinotte, 2011): Atlantis

113 Bank, Sapmer Bank, Middle of What Seamount, Melville Bank and Coral Seamount. The

114 SWIR is crossed by subtropical and Agulhas Return Current convergences (Figure 1). These

115 strong hydrological discontinuities are almost impassable by small size organisms, both in the

116 adult and larval stages. There is therefore no genetic connectivity between populations north

117 and south of the subtropical convergence line (Rogers, 2012). We include three other

118 seamounts located on the Madagascar Ridge: two unnamed pinnacles – hereafter called

119 MAD-Ridge and Un-named seamount respectively) and Walters Shoal. The rugged

120 topography and numerous shoals on this portion of the Madagascar Ridge interact with ocean

121 currents (Roberts et al., 2020, this issue; Vianello et al., 2020, this issue). MAD-Ridge is a

122 steep pinnacle (33 km north–south; 22 km east–west) located 240 km south of Madagascar

123 and rises to 240 m below the surface. It is under the influence of a highly dynamic ocean

124 circulation (the East Madagascar Current and its retroflection, Figure 1; de Ruijter et al.,

125   2004) inducing strong mesoscale activity (Pollard and Read, 2017; Vianello et al., 2020, this

126   issue). Indeed, it is frequently crossed by mesoscale eddies spinning off the South East

127   Madagascar Current. These eddies may become trapped over the seamount and have an

128   influence on the assemblages and diel vertical migrations patterns of micronekton

129   communities (Annasawmy et al., 2020, this issue). Walters Shoal and Un-named seamount

130   are very isolated features (>800 km south of Madagascar, 1300 km off the South African

131   coastline) located at the southern end of the Madagascar Ridge. Both seamounts are classified

132   as Benthic Protected Areas by the Southern Indian Ocean Fisheries Agreement (Shotton,

133   2006; SIOFA, 2019). Walters Shoal is a large seamount rising to 18 m below the surface

134   located 855 km south of Madagascar. Previous investigation showed a 400 km^2 caldera-like

135   shape of the summit (RV Marion Dufresne cruises in 1973 and 1976, unpublished data). It has

136   moderate mesoscale dynamics (Pollard and Read, 2017). The last seamount considered, La

137   Pérouse, is located 160 km northwest of La Réunion Island. It is under the influence of the

138   west-flowing South Equatorial Current (SEC, Figure 1) (Tomczak and Godfrey, 2003;

139   Chapman et al., 2003) and has moderate mesoscale dynamics. As an old volcano, La Pérouse

140   rises steeply to 55-60 m depth from the abyssal plain at 5000 m and is 10 km long (Marsac et

141   al., 2020, this issue).

142

143   We also considered eight coastal sites, where knowledge on species and/or circulation were

144   available, to assess exchanges with the seamounts: (i) two Mascarene archipelago sites, the

145   west coast of Mauritius (Morne Brabant) and La Réunion (La Saline); (ii) four sites in

146   Madagascar (Sainte-Marie and Mamanjary on the east coast, Fort-Dauphin in the south and

147   Tulear in the southwest); and (iii) two sites on the African coast (Tofo in Mozambique and

148   Saint Lucia in South Africa) (Figure 1). As these coastal sites are not fully representative of

149   the respective coastlines, we also defined buffers around countries (Mauritius, La Réunion,

150   Madagascar, Mozambique and South Africa), 1/3° from shore, to highlight larval export from

151   seamounts to surrounding countries.

152

153   The aim of this paper is to assess the degree of connectivity, deduced from hydrodynamic

154   larvae dispersion, between the nine selected SWIO seamounts and nearby coastal ecosystems

155   represented by the eight coastal sites and also nearby countries. Emphasis is placed on the

156   three shallow seamounts which are the focus of the present Special Issue: La Pérouse (LP –

157   doi:10.17600/16004500), MAD-Ridge (MR – doi:10.17600/16004900) and Walters Shoal

158   (WS – doi:10.17600/17002700) (Roberts et al., 2020, this issue). In order to characterize

159   connectivity patterns, we first used drifter trajectory data as evidence for possible

160   hydrodynamic connectivity. Then, to gain a broader view of connectivity patterns, we used

161   Ichthyop, a Lagrangian model (Lett et al., 2008) to simulate ichthyoplankton dispersal. This

162   model was forced by near-surface ocean current estimates (OSCAR). A wide range of PLD

163   values were considered to provide a synoptic view of seamount connectivity. Finally, we used

164   information on PLD and the age of larvae collected at MR and LP by Harris et al. (2020, this

165   issue) to assess their putative origin.

166

167   **2. Material and methods**

168   *2.1 SWIO marine species*

169   More than 800 fish species have been recorded on seamounts worldwide (Morato et al.,

170   2004). Most are robust demersal fish species, with good swimming capabilities, high food

171   consumption and energy expenditure. Some of them also exhibit great longevity (over 100

172   years) with late maturation (50-60 years) and low fertility, making them extremely vulnerable

173   to intensive fishing (Koslow et al., 2000).

174

175　Soviet and Ukrainian fisheries operating from 1969 to 1998 in the SWIO identified 81 fish

176　families including four *Beryx* species (alfonsinos, including *Beryx splendens* and *B.*

177　*decadactylus*) and orange roughy (*Hoplostethus atlanticus*) of high commercial value, pelagic

178　pentacerotidae (*Pseudopentaceros wheeleri*, *P. richardsoni*), rockfish (*Sebastes* spp.,

179　*Helicolenus* spp.), oreos (Oreosomatidae), cardinal fish (*Epigonus* spp.), grenadiers (including

180　*Coryphaenoides rupestris*) and Patagonian toothfish (*Dissostichus eleginoides*) (Romanov,

181　2003). These fish are specifically associated with seamounts, although they also live on the

182　continental slopes and slopes of oceanic islands. Soviet and Ukrainian fisheries also

183　inventoried a minimum of 13 threatened species of shark (Romanov, 2003) and benthic

184　resources such as crustaceans (lobsters, crabs), molluscs, sponges, and cold-water corals. A

185　new species of spiny lobster, *Palinurus barbarae* (Groeneveld et al., 2006), appears to be

186　endemic to the Walters Shoal (WS), as well as the crab *Beuroisia duhameli* (Guinot and

187　Richer de Forges, 1981) caught during the MD08 campaign of RV Marion-Dufresne in 1976.

188　More recently, cruises to La Pérouse (LP), MAD-Ridge (MR) and the WS seamounts allowed

189　identification of several micronekton species. Annasawmy et al. (2019) reported vertically

190　migrating common open-water species of gelatinous crustaceans, squid and fish concentrated

191　over the summit and flanks, and also an important community of seamount-

192　associated/resident fish. Harris et al. (2020, this issue) also collected mesopelagic fish larvae

193　during the current cruises, Myctophidae and Gonostomatidae being the most dominant

194　families at all three seamounts.

195

196　Despite these valuable recent data, biological data on marine species inhabiting SWIO

197　seamounts are generally lacking, as underlined in several publications (Rogers, 2012; FFEM,

198　2013; Rogers et al., 2017; Zucchi et al., 2018). In particular, there is only limited information

199　available on their PLD for ichthyological species recorded during sea campaigns (e.g.

200 *Pseudopentaceros richardsoni*, *Hoplostethus atlanticus*, *Beryx splendens*), which have PLDs

201 ranging from one to several months. Hence, *Beryx* spp. may have a PLD of around one year

202 (Shotton, 2016). *Jasus* spp. (spiny lobsters) were recorded in seamount habitats in the

203 southern hemisphere and are also known to have long PLDs. Hence, Booth (2006) reported

204 PLDs between 8 and 12 months for *J. verreauxi*, and between 12 and 24 months for *J.*

205 *edwardsii*. Harris et al. (2020, this issue) provided information on specimens collected at MR

206 of the acanthurid *Naso* sp. having a PLD of 84 d, *Labrid* spp. with a PLD of 26–28 d, *Apogon*

207 spp. with a PLD of 18–34 d and *Synodus sp.* with a PLD of 42 d (Stier et al., 2014). Thus, the

208 different species inhabiting the SWIO seamounts cover a large range of PLD values.

209

210 *2.2 Oceanographic drifter trajectories*

211 As a first approach to assessing dispersal and connectivity in the SWIO, we downloaded 6-h

212 interpolated trajectories of 1104 drogued oceanographic surface drifters located in the SWIO

213 over the period 15/02/1979 to 30/06/2018 from the Global Drifter Program database

214 (https://data.nodc.noaa.gov/cgi-bin/iso?id=gov.noaa.nodc:AOML-GDP,   Lumpkin   and

215 Centurioni, 2019). From that dataset, we selected drifters that came close (<50 or 100 km) to

216 one of the three focus seamounts (LP, MR and WS) and plotted their trajectories. We also

217 searched for drifters that came close to two of the same seamounts, as an indication of

218 possible hydrodynamic connectivity between seamounts.

219

220 *2.3 Ichthyop larval dispersal model*

221 To gain a broader perspective of dispersal and connectivity in the SWIO, we used the larval

222 dispersal tool Ichthyop, a free Lagrangian tool designed to study the effects of physical and

223 biological factors on ichthyoplankton dynamics (Lett et al., 2008). Ichthyop can integrate the

224 most important processes involved in the early life stages of marine larvae: spawning,

225 transport, behaviour, growth, mortality and settlement. As we wished to obtain a synoptic

226 view of connectivity patterns, rather than focus on a particular species, we used a large range

227 of PLD values (15, 30, 45, 60, 90, 120, 180, 270 and 360 d) and assumed that all seamounts

228 had habitats and populations capable of both producing and receiving larvae. This latter

229 assumption is supported by the findings of Harris et al. (2020, this issue) who reported all

230 developmental stages of oceanic and some neritic taxa from preflexion to postflexion at LP,

231 MR and WS, an indication that the corresponding species spawn in the vicinity of these

232 seamounts. We also assumed that larvae were transported passively depending only on

233 horizontal surface currents. The term "larvae" used in the modelling part of this paper really

234 stands for "virtual larvae" because there were no ground truth data to calibrate and validate

235 the model. Particles were released every 5 d over 9 years, i.e. 10 000 particles at each of the

236 considered release locations, a number that was shown to be large enough to provide precise

237 estimates of connectivity values (Andrello et al., 2013). Release locations (Figure 1) were the

238 nine SWIO seamounts and the eight coastal sites described in the introduction. Potential larval

239 destination areas were the nine SWIO seamounts, the eight coastal sites and the shorelines of

240 the five countries (Mauritius, La Réunion, Madagascar, Mozambique and South Africa;

241 Figure 1). Simulations were performed with two sizes of buffer around locations used as

242 release and destination areas, 1/3 of a degree and 1 degree.

243

244 As expected, the simulated values of connectivity were overall greater with a 1° buffer than

245 with a 1/3° buffer, but as the connectivity patterns (i.e. sites that are more/less retentive,

246 more/less connected, etc.) were similar, we only present the 1/3° case and refer the reader to

247 Appendix Figure E for the 1° buffer results. The Ichthyop model was forced by current fields

248 provided by the OSCAR product (see below) interpolated linearly at the location and time of

249 each larva, and their movement was solved using the Runge Kutta 4th order scheme, diffusion

250 being added with a dissipation rate $\varepsilon=1\ E^{-9}\ m^2\ s^{-3}$ (following Peliz et al., 2007).

251

252 *2.4 OSCAR current product*

253 OSCAR (Ocean Surface Current Analyses – Real Time) provides estimates of ocean near-

254 surface currents by combining satellite-derived altimetry observations (sea-surface height; e.g.

255 TOPEX/Poseidon), scatterometer data that estimate ocean wind vectors, and sea surface

256 temperature sensors (e.g. AVHRR). OSCAR provides more precise ocean current estimates

257 than those based exclusively on altimetry, particularly in the tropics, by combining

258 geostrophic shear dynamics, Ekman and Stommel transport and a complementary term of

259 surface buoyancy gradient (Bonjean and Lagerloef, 2002). Products are available worldwide

260 at 1/3° horizontal resolution every 5 d and represent currents at a depth of ~15 m. Here we

261 used the currents data for the SWIO (latitude 10–50°S, longitude 20–70°E) over the period

262 2010–2018, downloaded from the NASA data center website (ftp://podaac-

263 ftp.jpl.nasa.gov/allData/oscar/preview/L4/oscar_third_deg/). OSCAR products were validated

264 for the northern part of the Indian Ocean by Sikhakolli et al. (2013).

265

266 *2.5 Model outputs and post-processing*

267 We calculated connectivity matrices between seamounts, between seamounts and coastal

268 ecosystems, and between coastal ecosystems and seamounts for all the considered PLD values

269 averaged over all release dates. Connectivity can be interpreted as either the proportion of

270 larvae exported to each seamount or coastal ecosystem (larval export, lines of the connectivity

271 matrices), or the proportion of larvae coming from each seamount or coastal ecosystem (larval

272 import, columns of the connectivity matrices). Local retention, i.e. the proportion of released

273 larvae that stayed at their natal sites, is the diagonal of the connectivity matrices. We also

11

274   computed the dispersal distance as the "great-circle distance" between the initial and final

275   positions of larvae, averaged for all larvae and release dates. We plotted maps of simulated

276   larval density, the average number of all larvae per cell at a given time. The cell size was set

277   as 1/3°, equivalent to the OSCAR resolution. Analyses were carried out using the software

278   ArGIS 10.4.1 and Spyder (Python 2.7).

279

280   **3. Results**

281

282   *3.1 Drifters*

283   We found 13, 11, and 14 drifters passing less than <50 km from the LP, MR and WS

284   seamounts, respectively, at some time in their travel in the SWIO (Figure 2). Most (11/13)

285   drifters that came close to LP ended up to the south in the direction of the other seamounts

286   (Figure 2a). One drifter (#45958) that came very close to LP (~ 7 km) was also close to MR

287   (~ 8 km) 85 d later (the trajectory of that drifter is highlighted by a white background in

288   Figure 2a). Drifters that travelled close to MR moved to the west or to the east and none

289   travelled to LP or WS (Figure 2b). Most (10/14) drifters that came close to WS ended up to

290   the west (Figure 2c), but along the way one drifter (#63941330) came close (~ 43 km) to MR

291   after 75 d (the trajectory of that drifter is highlighted by a white background in Figure 2c).

292

293   We found 32, 23 and 21 drifters that travelled <100 km from LP, MR and WS, respectively

294   (Appendix Figure A). Among those, six drifters came close to LP and then MR (with 46–189

295   d spent in between), two drifters travelled close to MR and then WS (29 and 70 d spent in

296   between) and two drifters came close to WS and then MR (75 and 143 d spent in between).

297   One of those drifters (#9108691) is of particular interest because it came close to first LP (~51

298   km), then MR (~71 km) and finally WS (~18 km), and was the fastest drifter, travelling from

12

299 LP to MR in 46 d and from MR to WS in 29 d (the trajectory of that drifter is highlighted by a

300 white background in Appendix Figure A).

301

302 *3.2 Mean dispersal distances*

303 In the simulations, as expected, the mean dispersal distances travelled by the virtual larvae

304 leaving seamounts increased with PLD, ranging from 217 km for PLD = 15 d to 1366 km for

305 PLD = 360 d, all seamounts averaged (Table 1). Larvae leaving Atlantis Bank had the shortest

306 average dispersal distances (around 0.6 times less than the mean) except for PLD = 15, where

307 the shortest distance was for larvae leaving WS (Table 1). Conversely, larvae from Coral

308 Seamount had the highest mean dispersal distances for all PLD (1.5–2.15 times above the

309 mean). For the three focal seamounts, larvae released from WS travelled the shortest average

310 distances, whereas larvae leaving MR travelled farthest.

311

312 *3.3 Connectivity matrices between all sites*

313 Matrices presented in Figure 3 show the mean simulated larval connectivity obtained between

314 all nine seamounts and eight coastal sites for three of the considered PLD values: 15, 120 and

315 360 d (matrices for the six other PLD values are provided in Appendix Figure B). For a PLD

316 of 15 d (Figure 3a), there were bilateral exchanges between Morne Brabant (Mauritius coastal

317 site), La Saline (La Réunion coastal site) and LP, one of our three focal seamounts. For the

318 other two seamounts, there was also bilateral exchange between WS and Un-named Seamount

319 (which are close) and between MR and Fort Dauphin. The highest local retention values were

320 for WS (11.1%), Atlantis Bank (7.5%) and LP (5.3%), in decreasing order. For a PLD of 120

321 d (Figure 3b), there was bilateral connectivity between the five sites situated East of

322 Madagascar (Maurice, La Réunion, LP, Mamanjary, Ile Ste Marie) and most of the seven sites

323 located south of Madagascar and in the Mozambique Channel (WS, Un-named Seamount,

13

324   MR, Fort Dauphin, Tulear, Tofo, Saint Lucia). Finally, there was connectivity between most

325   of the five seamounts situated on the SWIR (Atlantis Bank, Sapmer Bank, Middle of What

326   Seamount, Melville Bank, Coral Seamount), attaining an elevated degree between Sapmer

327   Bank, Middle of What seamount and Melville Bank. There was also bilateral exchange

328   between WS and MR, LP and MR, and WS and LP. For a PLD of 360 d (Figure 3c), most

329   sites were connected in both directions to some extent: the SWIR and South Madagascar

330   seamounts group tended to join. WS, MR and LP were connected bilaterally to all seamounts

331   and coastal sites, with the sole exception of LP which did not receive any larva from Saint

332   Lucia. We assessed the temporal variability (seasonal and interannual combined) of simulated

333   connectivity for the different PLD values (Appendix Figure C) and obtained little variability

334   with coefficients of variation (CV) of 2.7 at most. The CV tended to decrease with PLD, and

335   to have similar values for seamounts within the three different identified groups, i.e. east

336   Madagascar, south Madagascar and Mozambique Channel, and SWIR, and also between two

337   different groups (hence the "blocks" of similar colours in Appendix Figure Cc).

338

339   *3.4 Connectivity matrices between LP, MR and WS seamounts and coastal ecosystems*

340   Figure 4 represents exchanges from seamounts to coastal ecosystems (coastal buffers) for

341   PLD values of 15, 120 and 360 d (matrices for the six other PLD values are in Appendix

342   Figure D).

343   After 15 d of dispersal, connectivity ranged from 0 to 2.1%. Larvae released at LP reached the

344   coastal ecosystems of Mauritius (0.007%), Madagascar (0.03%) and La Réunion (2.1%),

345   whereas larvae from MR only reached Madagascar. After 120 d, larval connectivity values

346   were divided by ~5, ranging between 0 and 0.42%. Larvae from LP reached all coastal

347   ecosystems (Mauritius, La Réunion, Madagascar, Mozambique and South Africa). The two

348   highest connectivity values were between LP and Madagascar (0.42%) and between LP and

349 La Réunion (0.21%). Larvae from MR also reached all coastal ecosystems, but with lower

350 connectivity values. Larvae from WS reached all coastal ecosystems except Mauritius, with

351 even lower connectivity values. After 360 d of dispersal, larval connectivity values were

352 divided by ~10 relative to PLD = 120 d. All larvae leaving LP, MR and WS reached all

353 coastal ecosystems. Overall, the lowest connectivity was from WS, except to Mozambique

354 where it was the highest.

355

356 *3.5 Larval dispersal from LP, MR and WS*

357 The patterns of weak connectivity between seamounts and the coast described above result

358 from a high degree of dispersal towards offshore locations, as shown by maps of larval

359 density over the entire region. Figure 5 presents mean larval density maps for larvae released

360 at LP, MR and WS seamounts after 15, 120 and 360 d of PLD (with the locations of the

361 drifters of Figure 2 superimposed). Larvae released from LP remained concentrated at high

362 density on the eastern side of Madagascar for a PLD of up to 120 d, and then tended to drift

363 east. After 120 d, larvae released at MR split into two separate plumes, one directed east and

364 the other west towards the South African coast. Larvae released at WS remained concentrated

365 around that seamount for a longer time, eventually spreading east and west, similarly to larvae

366 released at MR.

367

368 *3.6 Local retention and connectivity between LP, MR, and WS*

369 Local retention decreased with increasing PLD for all three seamounts, but at a faster rate for

370 LP than for MR and WS (Figure 6). Conversely, connectivity between pairs of seamounts

371 initially increased with increasing PLD values (Figure 7). Patterns of connectivity change

372 with PLD and were similar for MR to WS, MR to LP, and WS to MR, first increasing

373 strongly, then peaking around 120 d and eventually decreasing slightly for longer PLDs.

374 Connectivity between the most distant sites, WS and LP, was much weaker and continued to

375 increase with PLD in the range of values tested. Connectivity from LP to MR was at an

376 intermediate level and showed the least change with PLD.

377

378 *3.7 Larval import at LP, MR and WS*

379 The origin of larvae reaching LP, MR and WS is shown in Figure 8 after PLDs of 15, 120,

380 and 360 d. At 15 d, larvae reaching WS, MR and LP were mostly self-recruits (95%, 95% and

381 77%, respectively). For a PLD of 120 d, there was still a lot of self-recruitment at WS (42%)

382 and MR (38%), but not at LP (15%), at which 57% of larvae came from Madagascar. At 360

383 d, there was still 27% of self-recruitment on WS and no larvae coming from LP. The pattern

384 was similar for MR, but with only 17% of self-recruitment. For LP, there was only 9% of self-

385 recruitment, with the balance of larvae originating from MR (15%), WS (2%), Mauritius and

386 La Réunion (20%), Madagascar (37%) and other seamounts (10%).

387

388 *3.8 Link with ichthyoplankton data*

389 It is difficult to interpret the above results in a biological sense because the larval durations of

390 the species inhabiting the seamounts are poorly known. However, Harris et al. (2020, this

391 issue) provide useful information on PLD and age for a set of larvae they collected at MR and

392 LP. In particular, at MR, they collected larvae of four species with estimated PLDs close to 30

393 d (*Labrid* and *Apogon* spp.), 45 d (*Synodus* sp.) and 90 d (the acanthurid *Naso* sp.). Assuming

394 that these species reproduce at all the sites under consideration, dispersal patterns can be

395 obtained for these PLD values (Figure 9) and also larval import and export for MR, where

396 most larvae were collected (Figure 10). For a PLD of 30 d, virtual larvae arriving at MR

397 originated from Fort Dauphin, MR and Un-named seamount (Figure 10). For a PLD of 45 d,

398 virtual larvae arriving at MR originated from Saint Lucia, Tofo, Fort Dauphin, MR, Un-

399 named seamount and WS. For a PLD of 90 d, they originated from all 17 release sites.

400

401 Harris et al. (2020, this issue) also provide age estimates for some of the larvae they collected.

402 All larvae collected at MR were in the range 1.4-16.2 d, a range is largely consistent with the

403 ages of virtual larvae transported from Fort Dauphin to MR in our simulations (Figure 11a).

404 Ages of virtual larvae transported from Mamanjary to MR (>10 d, Figure 11b) suggest that

405 the oldest larvae collected, such as *Synodus* and *Trachinocephalus myops*, may also have been

406 transported from there. At LP, all larvae collected except one (a macrourid species) have

407 estimated ages >5 d and may therefore have been transported from La Saline (Figure 11c),

408 whereas collected larvae >10 d (*Vinciguerria* spp.) may also have come from Morne Brabant

409 (Figure 11d). Of course, all larvae collected could also have been self-recruits.

410

411 **4. Discussion and perspectives**

412 The aim of this work was to assess the degree of connectivity between nine seamounts of the

413 South West Indian Ocean (SWIO) and nearby coastal ecosystems, with emphasis on three

414 shallow seamounts: La Pérouse (LP), MAD-Ridge (MR) and Walters Shoal (WS). The

415 Lagrangian model of larval dispersal allowed us to explore a wide range of pelagic larval

416 durations (PLDs) and revealed robust patterns of larval connectivity.

417

418 *4.1 Mean drift velocities and larval dispersal distance*

419 Larvae dispersed far from their site of origin, with travelled distances increasing with PLD.

420 Mean drift velocities, obtained by dividing the mean larval distances reported in Table 1 by

421 PLD, reached values as high as 10 km d^{-1} (about 0.1 m s^{-1}). Such values are consistent with

422 current surface velocities found by Pollard and Read (2017) and Vianello et al. (2020, this

423   issue) during the MAD-Ridge cruise. They are also of the same order of magnitude as other

424   estimates obtained by Lagrangian simulations in other regions. For example, median drift

425   velocities were about 4 km d^{-1} in the Mediterranean Sea (Andrello et al., 2013). Other

426   connectivity studies performed in the SWIO have highlighted long-distance colonization,

427   possibly over several generations, between coral reefs (Crochelet et al., 2016), between South

428   African ecosystems and La Réunion for vagrant dusky groupers (Reid et al., 2016), between

429   Mauritius and La Réunion for honeycomb groupers (Crochelet et al., 2013), between the

430   Mascarene archipelago and Madagascar for tropical eel (Pous et al., 2010) and Seychelles for

431   Sargassum algae (Mattio et al., 2013), between the east African coast and Madagascar for

432   mangrove propagules (Van der Stocken and Menemenlis, 2017) and for coral reef species

433   (Gamoyo et al., 2019; Schleyer et al., 2019), and between ABNJ (Areas Beyond National

434   Jurisdiction) and coastal zones (Popova et al., 2019, Maina et al., 2020). Our results focusing

435   on seamounts show that currents around SWIO seamounts can be powerful means of larval

436   dispersal over relatively long distances. The longest dispersal distances were obtained from

437   the Coral Seamount, the southernmost seamount considered in this study, which is affected by

438   the strong current velocities of the Agulhas Return Current.

439

440   *4.2 Potential colonization of coastal sites by larvae originating from seamounts*

441   Connectivity from seamounts to coastal ecosystems was weak, with a maximum of 2.1%

442   larvae originating from seamounts reaching coastal ecosystems. It is difficult to conclude

443   whether such a low percentage of dispersal is good enough to influence the communities of

444   the receiving sites, because the magnitude of immigration depends on survival during the

445   pelagic phase and on local dynamics (Armsworth, 2002; Burgess et al., 2014). If a population

446   is not self-sustaining as a consequence of high mortality or low fecundity rates, then

447   immigration from other populations contributes to population persistence. Although some of

18

448   the seamounts mentioned herein are subject to fishing (with strong impacts on stocks of long-

449   living species), coastal ecosystems are affected by greater anthropogenic pressure (e.g.

450   fishing, dredging, pollution) and generally have smaller biomasses than isolated sites (Edgar

451   et al., 2014; Cinner et al., 2016). Therefore, seamounts could be important sources of larvae

452   for coastal sites, if connectivity is strong enough to transport sufficiently high numbers of

453   larvae over long oceanic distances and the receiving habitat is appropriate. Owing to the lack

454   of data on local population dynamics and abundance in both the seamounts of origin and the

455   coastal sites of destination, however, this hypothesis cannot be tested here.

456

457   *4.3 Local retention at seamounts and connectivity between seamounts*

458   Local retention (within a 1/3° buffer) at the three focal seamounts (LP, MR and WS) was also

459   low, peaking at about 11.1% at the shortest PLD and decreasing sharply at longer PLDs.

460   These values may be an underestimation of actual patterns of local retention, however,

461   because of the relatively coarse spatial resolution of the ocean current product (OSCAR) and,

462   perhaps more importantly, the assumption of passive larval dispersal, because active

463   swimming and larval orientation mechanisms can increase local retention (Faillettaz et al.,

464   2018). Even if retention probabilities seem low, though, they might be sufficiently high to

465   replenish populations and ensure their persistence because of high fecundities of the fish

466   species. For example, large female alfonsino (*Beryx splendens*) spawn a range of 0.8–2.4

467   million eggs (Alekseeva, 1983). We also found that local retention was greater at WS than at

468   MR (Figure 6), which is consistent with Vianello et al. (2020, this issue) showing that

469   currents decrease from north to south along a transect going from MR to WS.

470

471   Maina et al. (2020) recently used a modelling approach similar to the one used here to assess

472   connectivity between seamounts of the SWIO using a PLD of 30 d. Here, we used a range of

19

473   PLD values from 15 to 360 d and showed that connectivity patterns change dramatically with

474   PLD. Here we obtained large differences in dispersal and connectivity patterns for PLD

475   values of 30, 45 and 90 d, which correspond broadly to labrid and *Apogon* spp., *Synodus* sp.,

476   and acanthurid *Naso* sp., respectively, collected by Harris et al. (2020, this issue) at MR

477   (Figure 10). Therefore, differences in the putative origin of these collected larvae were

478   significant (Figure 9), although a local (i.e. MR) origin was the most likely for all of them.

479   For some species, the presence of larvae, juveniles and adults around the same seamount

480   suggests that their populations are self-sustaining (Cherel et al., 2020, this issue). For neritic

481   reef-associated species, it is also plausible that some of the larvae collected at MR originated

482   from the south-east coast of Madagascar (Harris et al., 2020, this issue). Indeed, MR has a

483   strong connection with the shelf waters through cross-shelf transport. This suggestion is

484   supported by our age analysis of larvae, which shows that larvae arriving at MR may come

485   from Fort Dauphin or Mamanjary (Figure 11). Similarly, it is also possible that larvae

486   collected at LP come from the islands of La Réunion and Mauritius (Figure 11).

487

488   Connectivity patterns between seamounts revealed three groups of greater connectivity: the

489   region between the eastern coast of Madagascar, Mauritius and La Réunion islands; the

490   seamounts of the SWIR; and the pair Walters Shoal – Un-named seamount. Connectivity

491   between these three groups was only at long PLDs.

492

493   With the exception of the two lowest connectivity values (between WS and LP), connectivity

494   peaked at around 120 d PLD and remained stable or slightly decreased at longer PLDs (Figure

495   7). However, that pattern does not consider the effects of larval mortality, which are likely to

496   reduce connectivity proportionally to PLD.

497

498 We found little temporal variability in simulated connectivity patterns, which is consistent

499 with Vianello et al. (2020, this issue) who reported no clear seasonality or interannual

500 variability in currents along the Madagascar Ridge.

501

502 *4.4 Complementarity of drifter data and Lagrangian simulations*

503 Drifter data were used as ground-truth information of hydrodynamic dispersal and

504 connectivity, and they consolidated the results of Lagrangian modelling. Indeed, the

505 trajectories followed by drifters passing close to each of the three focal seamounts were

506 consistent with the general patterns followed by particles released there. In addition, we found

507 drifters passing LP and then MR, passing WS and then MR, and passing LP and then MR and

508 WS, which were also among the strongest connections found between seamounts in the

509 Lagrangian model (Figure 7). Besides this, the range of time spent by drifters travelling from

510 LP to MR (46–189 d) corresponded well with the PLD values for connectivity between these

511 seamounts in the model. The range of time spent by drifters between the other seamounts (29–

512 70 d from MR to WS, 75–143 d from WS to MR) were also consistent with the model results,

513 although slightly slower. However, we found no drifter passing MR and then LP, although

514 that is one of the strongest connections according to simulation results (Figure 7).

515

516 *4.5 Limitations of the modelling approach*

517 Numerical transport models are increasingly being used to determine patterns of larval

518 dispersal as well as connectivity between populations in the marine environment. Larval

519 dispersal simulations are relatively simple and quick to implement in any study region.

520 Indeed, data necessary for model input (coastline, release sites, etc.) are freely available

521 online at high resolutions. Nevertheless, the work accomplished during this study could be

522 improve by taking into account additional oceanographic and biological factors.

523

524   We used an ocean current product (OSCAR) that relies on remote-sensing data to force the

525   Lagrangian larval dispersal model. OSCAR currents are available globally and over long

526   periods of time. Despite their coarse spatial resolution (1/3°), OSCAR and other products

527   providing near-surface ocean current estimates have been shown to allow the simulation of

528   surface drifter trajectories with similar accuracies as outputs from oceanographic models of

529   similar spatial resolution (Liu et al., 2014; Amemou et al., submitted).

530

531   However, OSCAR does not take into account the vertical stratification of currents in the water

532   column, which may affect larval dispersal patterns. In this study, larvae were considered as

533   passive particles drifting in the surface layer, because we had no knowledge of the larval

534   biology of local species. However, the larvae of many species have good swimming ability

535   (Fisher et al., 2005) and are capable of changing their behaviour (e.g. by changing their depth)

536   in response to the environment (Leis and Carson-Ewart, 2002; Tolimieri et al., 2000). This

537   affects how larvae are carried by currents (Irisson et al., 2010; Cherubin et al., 2011), because

538   transport is usually faster close to the surface than in the deeper layers. Larvae might therefore

539   rely on vertical migration to reduce their dispersal and promote local retention (Cowen, 2002).

540   When such information is available, it is therefore important to consider larval behaviour and

541   swimming capability during larval ontogeny (Leis, 2010), and physical data such as vertical

542   stratification of currents.

543

544   Vianello et al. (2020, this issue) reported no clear seasonality or interannual variability in

545   currents along the Madagascar Ridge. Nevertheless, Annasawmy et al. (2019) highlighted a

546   strong seasonality in primary productivity at LP and MR, with maximum values reached in

547   July, as a result of intense mixing caused by the austral winter trade winds, and minimum

548   values during the austral summer (December–March). Moreover, chlorophyll a (Chl-a)

549   concentrations were twice as high at MR than at LP all year round. This seasonality and the

550   differences between seamounts may have consequences on secondary productivity and thus

551   on food availability, growth and survival for larvae. Harris et al. (2020, this issue) also

552   showed that different environmental variables such as temperature, Mixed Layer Depth

553   (MLD), Depth of Chlorophyll Maximum (DCM), zooplankton settled volume and integrated

554   Chl-a, influence larval fish communities at LP, MR and WS. Therefore, environmental factors

555   and their effect on biological processes such as larval growth and mortality are important

556   factors to consider in future modelling studies.

557

558   *4.6 Perspectives*

559   From the perspective of the conservation and management of ecosystems, in particular in

560   areas beyond national jurisdiction (ABNJ) where most SWIO seamounts are located,

561   improving the understanding and knowledge of larval dispersal is crucial. A new, legally

562   binding instrument for the high seas has been discussed since 2006 under the United Nations

563   Convention on the Law of the Sea for the conservation and sustainable use of marine

564   resources beyond national jurisdiction. Larval dispersal will be a key point in designing

565   regional networks of Marine Protected Areas (Andrello et al., 2017) to conserve biodiversity

566   in the high seas efficiently. Studies using numerical models in combination with the data and

567   knowledge gathered during at-sea expeditions could make a vital contribution to these efforts.

568   Indeed, genetic data could be gathered for several species covering a range of PLD values in

569   order to corroborate the connectivity patterns simulated here between seamounts. In addition,

570   behavioural data such as larval and adult mobility, and demographic data including egg

571   production and pre- and post-settlement mortality, should also be considered, because these

23

572   factors are as critical information as connectivity in determining the dynamics of populations,

573   and therefore their persistence.

574

575 Fig. 1. Main currents of the SWIO obtained from OSCAR current data averaged over the

576 period 2010–2017, and the location of the nine studied seamounts, the eight coastal sites and

577 surrounding countries (buffers).

578

579 Fig. 2. Trajectories of drifters passing less than 50 km from (a) La Pérouse, (b) MAD-Ridge

580 and (c) Walters Shoal during their drift in the SWIO. Small white circles show the closest

581 locations of drifters to seamounts used as the start of the represented trajectories, and small

582 black circles are the final locations.

583

584 Fig. 3. Connectivity matrices between all seamounts and coastal sites for PLDs of (a) 15, (b)

585 120 and (c) 360 d. The values represent the percentage of larvae released at each release site

586 transported to each destination site at the given PLD. The cells in the diagonal of the matrices

587 are values of local retention. White = no connectivity (0%). Note that the colour scale differs

588 between panels.

589

590 Fig. 4. Connectivity matrices between seamounts and coastal ecosystems for PLDs of (a) 15,

591 (b) 120 and (c) 360 d. The values represent the percentage of larvae released at each release

592 site transported to each destination site at the given PLD. The cells in the diagonal of the

593 matrices are values of local retention. White = no connectivity (0%). Note that the colour

594 scale differs between panels.

595

596 Fig. 5. Maps of average density for virtual larvae released at La Pérouse (a, d, g), MAD-Ridge

597 (b, e, h) and Walters Shoal (c, f, i) for PLDs of 15, 120 and 360 d. Pink dots are the locations

25

598   of the drifters shown in Figure 2 at the same time (i.e. 15, 120 and 360 d after they passed less

599   than 50 km from the seamount).

600

601   Fig. 6. Local retention (%) at La Pérouse, MAD-Ridge and Walters Shoal for PLDs of 15, 30,

602   45, 90, 120 180, 270 and 360 d.

603

604   Fig. 7. Connectivity (%) between La Pérouse, MAD-Ridge and Walters Shoal for PLDs of 15,

605   30, 45, 90, 120, 180, 270 and 360 d.

606

607   Fig. 8. Origin of the larvae reaching La Pérouse, MAD-Ridge and Walters Shoal for PLDs of

608   (a) 15, (b) 120 and (c) 360 d.

609

610   Fig. 9. Maps of average density for virtual larvae released at all seamounts and coastal sites

611   for PLDs of (a) 30, (b) 45 and (c) 90 d. These PLD correspond broadly to labrid and *Apogon*

612   *spp*., *Synodus* sp., and the acanthurid *Naso* sp., respectively.

613

614   Fig. 10. Origin of larvae reaching MAD-Ridge (imports) for PLDs of (a) 30, (b) 45 and (c) 90

615   d, and the destination of larvae leaving MAD-Ridge (exports) for PLDs of (d) 30, (e) 45 and

616   (f) 90 d. These PLD correspond broadly to labrid and *Apogon* spp., *Synodus* sp., and

617   acanthurid *Naso* sp., respectively.

618

619   Fig. 11. Age distributions of virtual larvae arriving at MAD-Ridge from (a) Fort Dauphin and

620   (b) Mamanjary, and arriving at La Pérouse from (c) La Saline and (d) Morne Brabant.

621

622 Table 1. Mean distances of larval dispersal (km) from each seamount for different Pelagic

623 Larval Durations (PLDs).

FROM \ PLD	15	30	45	60	90	120	180	270	360
La Pérouse	167	283	355	423	540	628	793	1031	1284
MAD-Ridge	337	460	575	665	804	901	1086	1368	1544
Walters Shoal	109	217	296	348	439	517	678	869	1014
Atlantis Bank	125	211	266	302	370	431	542	699	844
Sapmer Bank	164	236	292	356	443	530	674	854	1027
Middle of What Seamount	205	348	473	555	664	754	891	1061	1233
Coral Seamount	342	605	847	1070	1459	1718	2086	2393	2587
Melville Bank	311	551	719	830	979	1080	1256	1465	1638
Un-named Seamount	195	279	394	452	523	622	782	974	1122
Mean	**217**	**354**	**469**	**556**	**691**	**798**	**976**	**1190**	**1366**

624

625

626 Appendix Fig. A. Trajectories of drifters passing <100 km from (a) La Pérouse, (b) MAD-

627 Ridge and (c) Walters Shoal during their drift in the SWIO. Small white circles show the

628 closest locations of drifters to seamounts used as the start of the represented trajectories, and

629 small black circles are the final locations.

630

631 Appendix Fig. B. Connectivity matrices between all seamounts and coastal sites for PLDs of

632 (a) 30, (b) 45, (c) 60, (d) 90, (e) 180 and (f) 270 d. The values represent the percentage of

633 larvae released at each release site transported to each destination site at the given PLD. The

634 cells in the diagonal of the matrices are values of local retention. White = no connectivity

635 (0%). Note that the colour scale differs between panels.

636

637 Appendix Fig. C. Variability (seasonal and interannual combined) of simulated connectivity

638 for PLDs of (a) 15, (b) 120 and (c) 360 d. CV is the relative standard deviation (ratio of the

639 standard deviation to the mean).

640

641 Appendix Fig. D. Connectivity matrices between seamounts and coastal ecosystems for PLDs

642 of (a) 30, (b) 45, (c) 60, (d) 90, (e) 180 and (f) 270 d. The values represent the percentage of

643 larvae released at each release site and transported to each destination site at the given PLD.

644 The cells in the diagonal of the matrices are values of local retention. White = no connectivity

645 (0%). Note that the colour scale differs between panels.

646

647 Appendix Fig. E. Connectivity matrices between all seamounts and coastal sites for all PLDs.

648 The buffer used around all release and destination sites was 1° (instead of the 1/3° in Fig. 3

649 and Appendix Fig. B). The values represent the percentage of larvae released at each release

650 site transported to each destination site at the given PLD. The cells in the diagonal of the

28

651   matrices are values of local retention. White = no connectivity (0%). Note that the colour

652   scale differs between panels.

653

654   **References**

655   Alekseeva, E.I., 1983. Maturation of ovaries, nature of spawning and local specific character
656   of genital cycles of alfonsino *Beryx splendens* Lowe from the Atlantic Ocean. In: Problems of
657   early ontogeny of fish – theses of reports, pp. 72–73. Kaliningrad, USSR, AtlantNIRO (in
658   Russian).

659

660   Amemou, H., Koné, V., Aman, A., Lett, C. (submitted) Assessment of a Lagrangian model
661   using trajectories of oceanographic drifters and fishing devices in the Tropical Atlantic Ocean.
662   Prog. Oceanogr.

663

664   Andrello, M., Guilhaumon, F., Albouy, C., Parravicini, V., Scholtens, J., Verley, P., Barange,
665   M., Sumaila, U.R., Manel, S., Mouillot, D., 2017. Global mismatch between fishing
666   dependency and larval supply from marine reserves. Nature Comms 8, 16039.

667

668   Andrello, M., Mouillot, D., Beuvier, J., Albouy, C., Thuiller, W., Manel, S.. 2013. Low
669   connectivity between Mediterranean Marine Protected Areas: a biophysical modeling
670   approach for the dusky grouper Epinephelus marginatus. PLoS ONE 8, e68564.

671

672   Annasawmy, P., Ternon, J-F., Cotel, P., Cherel, Y., Romanov, E.V., Roudaut, G., Lebourges-
673   Dhaussy, A., Ménard, F., Marsac, F., 2019. Micronekton distributions and assemblages at two
674   shallow seamounts of the south-western Indian Ocean: Insights from acoustics and
675   mesopelagic trawl data, Prog. Oceanogr. 178, 102161. doi:10.1016/j.pocean.2019.102161

676

677   Annasawmy, P., Ternon, J-F., Lebourges-Dhaussy, A., Roudaut, G., Herbette, S., Ménard, F.,
678   Cotel, P., Marsac, F., 2020. Micronekton distribution as influenced by mesoscale eddies,
679   Madagascar shelf and shallow seamounts in the south-western Indian Ocean: an acoustic
680   approach. Deep-Sea Res. II. (this issue).

681

682   Armsworth, P.R. 2002. Recruitment limitation, population regulation, and larval connectivity
683   in reef fish metapopulations. Ecology 83, 1092–1104.

684

685   Boehlert, G.W., Watson, W., Sun, L.C., 1992. Horizontal and vertical distributions of larval
686   fishes around an isolated oceanic island in the tropical Pacific. Deep Sea Res. A.
687   Oceanographic Research Papers, 39(3–4), 439-466.

688

689   Bonjean, F., Lagerloef, G.S.E., 2002. Diagnostic model and analysis of the surface currents in
690   the tropical Pacific Ocean. J. Phys. Oceanogr. 32(10), 2938-2954.

691

692   Booth, J.D., 2006. *Jasus* species. In: Phillips B.F. (ed.) Lobsters: Biology, Management,
693   Aquaculture and Fisheries. Blackwell Scientific, Oxford, pp 340–358.

694

695   Bryan-Brown, D.N., Brown, C.J., Hughes, J.M., Connolly, R.M., 2018. Patterns and trends in
696   marine population connectivity research. Mar. Ecol. Prog. Ser. 585, 243–256.
697   https://doi.org/10.3354/meps12418

698

699   Burgess, S.C., Nickols, K.J., Griesemer, C.D., Barnett, L.A., Dedrick, A.G., Satterthwaite,
700   E.V., et al., 2014. Beyond connectivity: how empirical methods can quantify population
701   persistence to improve marine protected-area design. Ecol. Appl. 24, 257–270. doi:
702   10.1890/13-0710.1.

703

704 Chapman, P., Marco, S.F.D., Davis, R., Coward, A., 2003. Flow at intermediate depths
705 around Madagascar based on ALACE float trajectories. Deep Sea Res. II: Topical Studies in
706 Oceanography 50, 1957–1986. doi:10.1016/S0967-0645(03)00040-7

707

708 Cherel, Y., Romanov, E.V., Annasawmy, P., Thibault, D., Ménard, F., 2020. Micronektonic
709 fish species over three seamounts in the southwestern Indian Ocean. Deep-Sea Res. II. (this
710 issue).

711

712 Cherubin, L.M., Nemeth, R.S., Idrisi, N., 2011. Flow and transport characteristics at an
713 *Epinephelus guttatus* (red hind grouper) spawning aggregation site in St Thomas (US Virgin
714 Islands). Ecol. Model. 222, 3132–3148. doi:10.1016/j.ecolmodel.2011.05.031

715

716 Cinner, J.E., Huchery, C., MacNeil, M.A., Graham, N.A.J., McClanahan, T.R., Maina, J., et
717 al., 2016. Bright spots among the world's coral reefs. Nature 535, 416–419.

718

719 Clark, M.R., Schlacher, T.., Rowden, A.A., Stocks, K.I., Consalvey, M., 2012. Science
720 priorities for seamounts: research links to conservation and management. PLoS ONE 7,
721 e29232, doi:10.1371.

722

723 Cowen, R.K., 2002. Larval dispersal and retention and consequences for population
724 connectivity. In: Sale, P.F. (ed.), Coral Reef Fishes: Dynamics and Diversity in a Complex
725 Ecosystem. Academic Press, London. pp. 149–170.

726

727 Cowen, R.K., Gawarkiewicz, G., Pineda, J., Thorrold, S., Werner, F., 2007. Population
728 connectivity in marine systems: an overview. Oceanography 20, 14–21.
729 https://doi.org/10.5670/oceanog.2007.26.

730

731 Cowen, R.K., Lwiza, K.M.M., Sponaugle, S., Paris, C.B., Olson, D.B., 2000. Connectivity of
732 marine populations: open or closed? Science 287, 857.

733

734 Crochelet, E., Chabanet, P., Pothin, K., Lagabrielle, E., Roberts, J., Pennober, G., Lecomte-
735 Finiger, R. and Petit, M., 2013. Validation of a fish larvae dispersal model with otolith data in
736 the western Indian Ocean and implications for marine spatial planning in data-poor regions.
737 Ocean Coast. Mgmt 86, pp.13-21.

738

739 Crochelet, E., Roberts, J., Lagabrielle, E., Obura, D., Petit, M., Chabanet, P., 2016. A model-
740 based assessment of reef larvae dispersal in the Western Indian Ocean reveals regional
741 connectivity patterns—potential implications for conservation policies. Reg Stud. Mar. Sci. 7,
742 pp.159-167.

743

744 de Ruijter, W.P.M., van Aken, H.M., Beier, E.J., Lutjeharms, J.R.E., Matano, R.P., Schouten,
745 M.W., Schlitzer, R., 2004. Eddies and dipoles around South Madagascar: formation, pathways
746 and large-scale impact. Deep Sea Res. 51, 383-400.

747

748 Doherty, P. J., Planes, S., Mather, P., 1995. Gene flow and larval duration in seven species of
749 fish from the Great Barrier Reef. Ecology, 76(8), 2373-2391.

750

751 Edgar, G.J., Stuart-Smith, R.D., Willis, T.J., Kininmonth, S., Baker, S.C., Banks, S., et al.,
752 2014. Global conservation outcomes depend on marine protected areas with five key features.
753 Nature 506, 216–220.
754
755 Faillettaz, R., Paris, C.B., Irisson, J-O., 2018. Larval fish swimming behavior alters dispersal
756 patterns from Marine Protected Areas in the North-Western Mediterranean Sea. Front. Mar.
757 Sci. 5, 97. doi: 10.3389/fmars.2018.00097
758
759 FAO, 2018. The State of World Fisheries and Aquaculture 2018 - Meeting the sustainable
760 development goals. Rome, FAO.
761
762 FFEM, 2013. Note d'Engagement de Projet (NEP). Conservation et exploitation durable des
763 écosystèmes de monts sous-marins et sources hydrothermales du Sud-Ouest de l'Océan Indien
764 au-delà des zones de juridiction nationale. 67 pp.
765
766 Fisher, R., Leis, J.M., Clark, D.L., Wilson, S.K., 2005. Critical swimming speeds of late-stage
767 coral reef fish larvae: variation within species, among species and between locations. Mar.
768 Biol. 147, 1201-1212.
769
770 Gamoyo, M., Obura, D., Reason, C.J.C., 2019. Estimating connectivity through larval
771 dispersal in the Western Indian Ocean. J. Geophys. Res. Biogeosci. 124, 2446–2459.
772 https://doi.org/10.1029/2019JG005128
773
774 Groeneveld, J.C., Griffiths, C.L., van Dalsen, A.P., 2006. A new species of spiny lobster,
775 *Palinurus barbarae* (Decapoda, Palinuridae) from Walters Shoals on the Madagascar Ridge.
776 Crustaceana 79(7), 821-823.
777
778 Guinot, D., Richer de Forges, B., 1981. Crabes de profondeur, nouveaux ou rares, de l'Indo-
779 Pacifique (Crustacea, Decapoda, Brachyura). Bulletin du Muséum national d'Histoire
780 naturelle, 1ère partie 4(2), 1113-1153. 2ème partie 4(3), 227-260.
781
782 Guinotte, J., 2011. Seamount map of the Indian Ocean. Marine Conservation Biology
783 Institute; 3 pp. http://www.savethehighseas.org/publicdocs/Indian-Ocean-map.pdf
784
785 Harris, S., Noyon, M., Roberts, M.J., Marsac, F., 2020. Ichthyoplankton assemblages at three
786 shallow seamounts in the South West Indian Ocean: La Pérouse, MAD-Ridge and Walters
787 Shoal. Deep-Sea Res. II. (this issue).
788
789 Hastings, A., Botsford, L.W., 2006. Persistence of spatial populations depends on returning
790 home. Proc. Natl Acad. Sci. 103, 6067–6072. doi: 10.1073/pnas.0506651103 PMID:
791 16608913
792
793 Hellberg, M.E., 2007. Footprints on water: the genetic wake of dispersal among reefs. Coral
794 Reefs 26, 463–473.
795
796 Irisson, J.O., Paris, C.B., Guigand, C.M., Planes, S., 2010. Vertical distribution and
797 ontogenetic 'migration' in coral reef fish larvae. Limnol. Oceanogr. 55, 909-919.
798

799   Jones, G.P., Almany, G.R., Russ, G.R., Sale, P.F., Steneck, R.S., van Oppen, M.J.H., et al.,
800   2009. Larval retention and connectivity among populations of corals and reef fishes: history,
801   advances and challenges. Coral Reefs 28, 307–325.

803   Kingsford, M.J., Leis, J.M., Shanks, A., Lindeman, K.C., Morgan, S.G., Pineda, J., 2002.
804   Sensory environments, larval abilities and local self-recruitment. Bull. Mar. Sci. 70, 309–340.

806   Koslow, J.A., Boehlert, G.W., Gordon, J.D.M., Haedrich, R.L., Lorance, P., Parin, N., 2000.
807   Continental slope and deep-sea fisheries: implications for a fragile ecosystem. ICES J. Mar.
808   Sci. 57, 548-557.

810   Leis, J.M., 1984. Larval fish dispersal and the east Pacific Barrier. Océanogr. Trop. 19, 181-
811   192.

813   Leis, J.M., 1991. The pelagic phase of coral reef fishes: larval biology of coral reef fishes. pp.
814   183–230. In: Sale, P.F. (ed.). The Ecology of Fishes on Coral Reefs, Academic Press, San
815   Diego. 754 pp.

817   Leis, J., 2002. Pacific coral-reef fishes: the implications of behaviour and ecology of larvae
818   for biodiversity and conservation, and a reassessment of the open population paradigm. Env.
819   Biol. Fish. 65, 199–208.

821   Leis, J., 2010. Ontogeny of behaviour in larvae of marine demersal fishes. Ichthyol. Res 57,
822   325–342. doi:10.1007/s10228-010-0177-z

824   Leis, J.M., Carson-Ewart, B.M., 2002. *In situ* settlement behaviour of damselfish
825   (Pomacentridae) larvae. J. Fish Biol. 61, 325-346.

827   Lett, C., Verley, P., Mullon, C., Parada, C., Brochier, T., Penven, P., Blanke, B., 2008. A
828   Lagrangian tool for modelling ichthyoplankton dynamics. Env. Model. Softw. 23, 1210–1214.
829   doi:10.1016/j.envsoft.2008.02.005

831   Liu, Y., Weisberg, R.H., Vignudelli, S., Mitchum, G.T., 2014. Evaluation of altimetry-derived
832   surface current products using Lagrangian drifter trajectories in the eastern Gulf of Mexico. J.
833   Geophys. Res.: Oceans 119, 2827–2842. https://doi.org/10.1002/2013JC009710.

835   Luiz, O.J., Allen, A.P., Robertson, D.R., Floeter, S.R., Kulbicki, M., Vigliola, L., Becheler,
836   R., Madin, J.S., 2013. Adult and larval traits as determinants of geographic range size among
837   tropical reef fishes. Proc. Nat. Acad. Sci., 110(41), 16498-16502.
838   https://doi.org/10.1073/pnas.1304074110

840   Lumpkin, R., Centurioni, L., 2019. Global Drifter Program quality-controlled 6-hour
841   interpolated data from ocean surface drifting buoys. NOAA National Centers for
842   Environmental Information. Dataset. https://doi.org/10.25921/7ntx-z961.

844   Maina, J.M., Gamoyo, M., Adams, V.M., D'agata, S., Bosire, J., Francis, J., Waruinge, D.,
845   2020. Aligning marine spatial conservation priorities with functional connectivity across
846   maritime jurisdictions. Conserv. Sci. Practice. https://doi.org/10.1111/csp2.156
847

848 Manel, S., Loiseau, N., Andrello, M., Fietz, K., Goñi, R., Forcada, A., Lenfant, P.,
849 Kininmonth, S., Marcos, C., Marques, V., Mallol, S., Pérez-Ruzafa, A., Breusing, C., Puebla,
850 O., Mouillot, D., 2019. Long-distance benefits of marine reserves: myth or reality? Trends
851 Ecol. Evol. 34, 342–354. https://doi.org/10.1016/j.tree.2019.01.002

853 Marsac, F., Annasawmy, P., Noyon, M., Demarcq, H., Soria, M., Rabearisoa, N., Bach, P.,
854 Cherel, Y., Grelet, J., Romanov, E.V. Physical environment and ecological interactions at and
855 near La Pérouse seamount, northwest of Réunion Island, Indian Ocean. Deep Sea Res. II (this
856 issue).

858 Mattio, L., Zubia, M., Loveday, B., Crochelet, E., Duong, N., Payri, C.E., Bhagooli, R.,
859 Bolton, J.J., 2013. Sargassum (Fucales, Phaeophyceae) in Mauritius and Réunion, western
860 Indian Ocean: taxonomic revision and biogeography using hydrodynamic dispersal models.
861 Phycologia 52, 578–594. https://doi.org/10.2216/13-150.1

863 Moberg, F., Folke, C., 1999. Ecological goods and services of coral reef ecosystems. Ecol.
864 Econ. 29, 215–233.

866 Mora, C., Treml, E.A., Roberts, J., Crosby, K., Roy, D., Tittensor, D.P., 2012. High
867 connectivity among habitats precludes the relationship between dispersal and range size in
868 tropical reef fishes. Ecography 35, 89–96. doi:10.1111/j.1600-0587.2011.06874.x

870 Morato, T., Cheung, W.W.L., Pitcher T.J., 2004. Addition to Froese and Sampang's checklist
871 of seamount fishes. In: Morato, T., Pauly, D. (eds). Seamounts: Biodiversity and Fisheries.
872 Fisheries Centre Research Reports, 12 (5), Appendix 1: 1-6. Fisheries Centre, University of
873 British Columbia, Canada.

875 Obura, D., 2012. The diversity and biogeography of Western Indian Ocean reef-building
876 corals. PLoS ONE 7(9), e45013. https://doi.org/10.1371/journal.pone.0045013

878 Peliz, A., Marchesiello, P., Dubert, J., Marta-Almeida, M., Roy, C., Queiroga, H., 2007. A
879 study of crab larvae dispersal on the western Iberian Shelf: physical processes. J. Mar. Syst.
880 68, 215–236.

882 Pineda, J., Reyns, N.B., Starczak, V.R., 2009. Complexity and simplification in understanding
883 recruitment in benthic populations. Pop. Ecol. 51, 17–32. DOI: 10.1007/s10144-008-0118-0

885 Planes, S., Doherty, P.J., Bernardi, G., 2001. Strong genetic divergence among populations of
886 a marine fish with limited dispersal, *Acanthochromis polyacanthus*, within the Great Barrier
887 Reef and the Coral Sea. Evolution 55, 2263-2273.

889 Pollard, R., Read, J., 2017. Circulation, stratification and seamounts in the Southwest Indian
890 Ocean. Deep Sea Res. Part II. Top. Stud. Oceanogr. 136, 36–43.
891 https://doi.org/10.1016/j.dsr2.2015.02.018.

893 Popova, E., Vousden, D., Sauer, W.H., Mohammed, E.Y., Allain, V., Downey-Breedt, N.,
894 Fletcher, R., Gjerde, K.M., Halpin, P.N., Kelly, S., Obura, D., 2019. Ecological connectivity
895 between the areas beyond national jurisdiction and coastal waters: safeguarding interests of
896 coastal communities in developing countries. Mar. Pol. 104, 90-102.
897

34

Pous, S., Feunteun, E., Ellien, C., 2010. Investigation of tropical eel spawning area in the South-Western Indian Ocean: influence of the oceanic circulation. Prog. Oceanogr. 86, 396–413. https://doi.org/10.1016/j.pocean.2010.06.002.

Read, J., Pollard, R., 2017. An introduction to the physical oceanography of six seamounts in the southwest Indian Ocean. Deep Sea Res. II: Topical Studies in Oceanography 136, 44–58. https://doi.org/10.1016/j.dsr2.2015.06.022.

Reid, K., Crochelet, E., Bloomer, P., Hoareau, T.B., 2016. Investigating the origin of vagrant dusky groupers, Epinephelus marginatus (Lowe, 1834), in coastal waters of Réunion Island. Mol. Phylogen. Evol. 103, 98-103.

Riginos, C., Victor, B.C., 2001. Larval spatial distributions and other early life–history characteristics predict genetic differentiation in eastern Pacific blennioid fishes. Proc. R. Soc. Lond.. Series B: Biological Sciences, 268(1479), 1931-1936.

Roberts, C.M., 1997. Connectivity and management of Caribbean coral reefs. Science 278, 1454–1457. doi:10.1126/science.278.5342.1454

Roberts, M.J., Ternon, J-F., Marsac, F., Noyon, M., 2020. The MAD-Ridge Project: bio-physical coupling around a shallow seamount on the northern Madagascar Ridge, Southwest Indian Ocean. Deep-Sea Res. II. (this issue).

Rogers, A.D., 2012. An Ecosystem Approach to Management of Seamounts in the Southern Indian Ocean. 1. Overview of Seamount Ecosystems and Biodiversity. IUCN, Gland, Switzerland. 60 pp.

Rogers, A.D., Alvheim, O., Bemanaja, E., Benivary, D., Boersch-Supan, P., Bornman, T.G., Cedras, R., Du Plessis, N., Gotheil, S., Høines, A., Kemp, K., Kristiansen, J., Letessier, T., Mangar, V., Mazungula, N., Mørk, T., Pinet, P., Pollard, R., Read, J., Sonnekus, T., 2017. Pelagic communities of the South West Indian Ocean seamounts: R/V Dr Fridtjof Nansen Cruise 2009-410. Deep-Sea Res. II: Topical Studies in Oceanography 136, 5–35. doi:10.1016/j.dsr2.2016.12.010

Romanov, E.V., 2003. Summary and review of Soviet and Ukrainian scientific and commercial fishing operations on the deepwater ridges of the Southern Indian Ocean. In: Romanov, E.V. (ed.). FAO Fish. Circ. 991, 84 pp.

Rowden, A.A., Dower, J.F., Schlacher, T.A., Consalvey, M., Clark, M.R., 2010. Paradigms in seamount ecology: fact, fiction, and future. Mar. Ecol. 31(Suppl. 1), 226–239.

Schleyer, M.H., Downey-Breedt, N.J., Benayahu, Y., 2019. Species composition of Alcyonacea (Octocorallia) on coral reefs at Europa Island and associated connectivity across the Mozambique Channel. Mar. Biodiv. 49, 2485–2491. https://doi.org/10.1007/s12526-019-00975-7.

Schultz, E.T., Cowen, R.K., 1994. Recruitment of coral reef fishes to Bermuda: lLcal retention or long-distance transport? Mar. Ecol. Prog. Ser. 109, 15–28.

947   Selkoe, K.A., Toonen, R.J., 2011. Marine connectivity: a new look at pelagic larval duration
948   and genetic metrics of dispersal. Mar. Ecol. Prog. Ser. 436, 291-305.
949
950   SIOFA, 2019. Report of the Fourth Session of the Scientific Committee (SC4), p. 195, 25- 29
951   March 2019, Yokohama.
952
953   Shotton, R., 2006. Management of demersal fisheries resources of the southern Indian Ocean.
954   FAO Fish. Circ. 1020, 90 pp.
955
956   Shotton, R., 2016. Global review of alfonsino (*Beryx* spp.), their fisheries, biology and
957   management. FAO Fish. Aquacult. Circ. C1084, 154 pp.
958
959   Sikhakolli, R., Sharma, R., Basu, S., Gohil, B.S., Sarkar, A., Prasad, K.V.S.R., 2013.
960   Evaluation of OSCAR ocean surface current product in the tropical Indian Ocean using in situ
961   data. J. Earth Syst. Sci. 122, 187–199. doi:10.1007/s12040-012-0258-7
962
963   Stier, A.C., Hein, A.N., Parravicini, V., Kulbicki, M., 2014. Larval dispersal drives trophic
964   structure across Pacific coral reefs. Nat. Comms, doi: 10.1038/ncomms6575
965
966   Tolimieri, N., Jeffs, A., Montgomery, J., 2000. Ambient sound as a cue for navigation by the
967   pelagic larvae of reef fishes. Mar. Ecol. Prog. Ser. 207, 219–224. doi:10.3354/meps207219
968
969   Tomczak, M., Godfrey, J.S., 2003. Regional Oceanography: an Introduction, 2nd edn. Daya
970   Publishing House, Delhi. 390 pp.
971
972   Treml, E.A., Halpin, P.N., Urban, D.L., Pratson, L.F., 2008. Modeling population
973   connectivity by ocean currents, a graph-theoretic approach for marine conservation.
974   Landscape Ecol. 23, 19–36.
975
976   UNEP-Nairobi Convention and WIOMSA (2015). The Regional State of the Coast Report:
977   Western Indian Ocean. UNEP and WIOMSA, Nairobi, Kenya, 546 pp.
978
979   Van der Stocken, T., Menemenlis, D., 2017. Modelling mangrove propagule dispersal
980   trajectories using high-resolution estimates of ocean surface winds and currents, Biotropica
981   49, 472–481. https://doi.org/10.1111/btp.12440.
982
983   Vianello, P., Herbette, S., Ternon, J-F., Demarcq, H., Roberts, M.J., 2020. Circulation and
984   hydrography in the vicinity of a shallow seamount on the northern Madagascar Ridge. Deep-
985   Sea Res. II. (this issue).
986
987   Victor, B.C., 1987. Growth, dispersal, and identification of planktonic labrid and pomacentrid
988   reef-fish larvae in the eastern Pacific Ocean. Mar. Biol. 95, 145–152.
989   doi:10.1007/BF00447496
990
991   Warner, R.R., Cowen, R.K., 2002. Local retention of production in marine populations:
992   evidence, mechanisms, and consequences. Bull. Mar. Sci. 70, 245-249.
993
994   Zucchi, S., Ternon, J-F., Demarcq, H., Ménard, F., Guduff, S., Spadone, A., 2018. Oasis for
995   marine life. State of knowledge on seamounts and hydrothermal vents. IUCN, Gland,

996 Switzerland, vi + 50 pp. ISBN: 978-2-8317-1934-4 (PDF). DOI:
997 10.2305/IUCN.CH.2018.14.en-fr
998

Table 1. Mean distances of larval dispersal (km) from each seamount for different Pelagic

Larval Durations (PLDs).

FROM \ PLD	15	30	45	60	90	120	180	270	360
La Perouse	167	283	355	423	540	628	793	1031	1284
MAD-Ridge	337	460	575	665	804	901	1086	1368	1544
Walters Shoal	109	217	296	348	439	517	678	869	1014
Atlantis Bank	125	211	266	302	370	431	542	699	844
Sapmer Bank	164	236	292	356	443	530	674	854	1027
Middle of What Seamount	205	348	473	555	664	754	891	1061	1233
Coral Seamount	342	605	847	1070	1459	1718	2086	2393	2587
Melville Bank	311	551	719	830	979	1080	1256	1465	1638
Un-named Seamount	195	279	394	452	523	622	782	974	1122
Mean	**217**	**354**	**469**	**556**	**691**	**798**	**976**	**1190**	**1366**

IMPORTS

Day 030 a) Day 045 b) Day 090 c)

EXPORTS

Day 030 d) Day 045 e) Day 090 f)

Seamounts of interest
■ MAD-Ridge   ■ La Perouse
■ Walters Shoal

Other seamounts
▦ Un-named Seamount
▨ Coral Seamount
≡ Melville Bank   Ⅲ Middle of What Seamount
▒ Sapmer Bank   ▧ Atlantis Bank

Madagascar sites
■ Tulear   ■ Fort Dauphin
■ Ile Ste Marie   ■ Mamanjary

Mascarene archipelago sites
■ Morne Brabant   ■ La Saline

East Africa sites
■ Santa Lucia   ■ Tofo

Source = Fort Dauphin, dest. = MAD-Ridge

a)

Source = Mamanjary, dest. = MAD-Ridge

b)

Source = La Saline, dest. = La Perouse

c)

Source = Morne Brabant, dest. = La Perouse

d)

Name	Summit depth (meters)
Atlantis Bank	690
Sapmer Bank	261
Middle of What Seamount	876
Coral Seamount	175
Melville Bank	91
Un-named Seamount	1249
Walter's Shoal	18
La Pérouse	55
MAD-Ridge	240
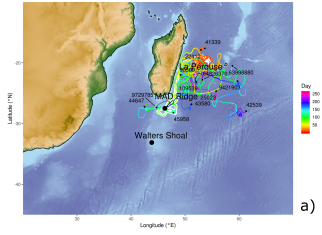
a)
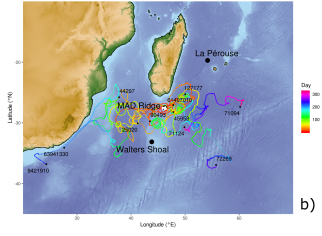
b)
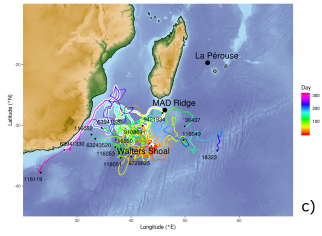
c)

La Pérouse   MAD-Ridge   Walters Shoal

a) Day 015

b) Day 120

c) Day 360

a)

Day 030

b)

Day 045

c)

Day 090

a)

b)

c)
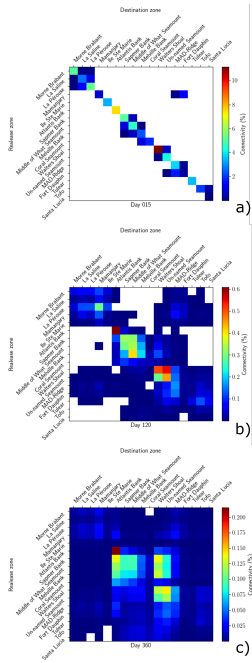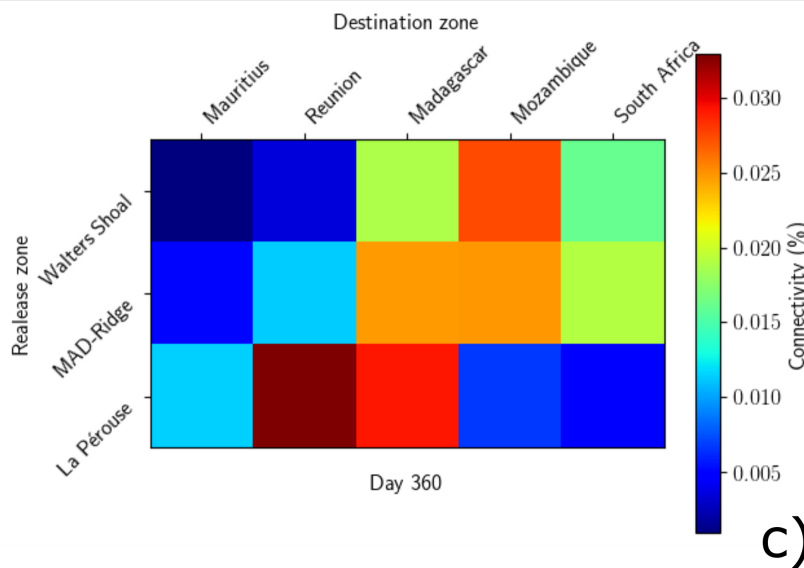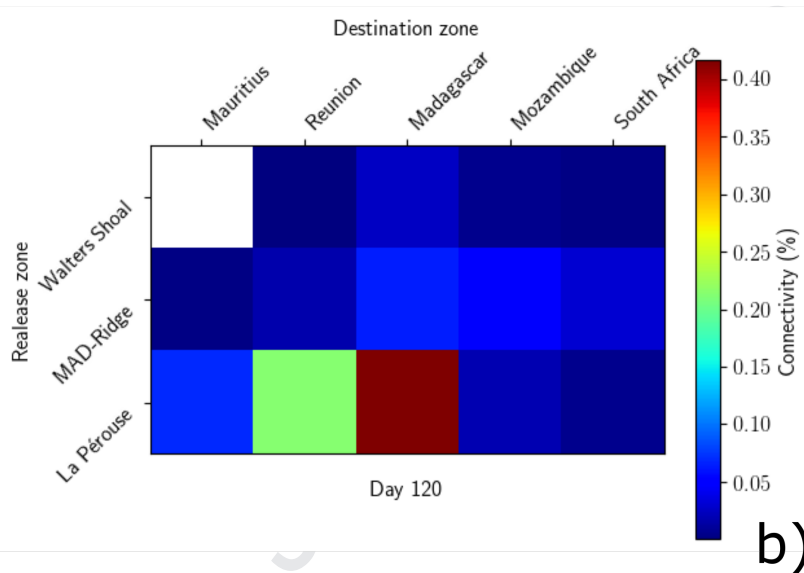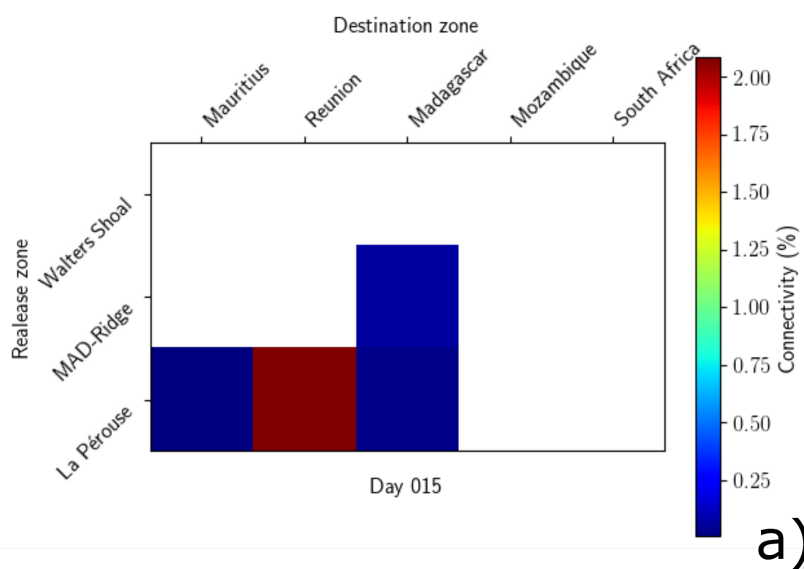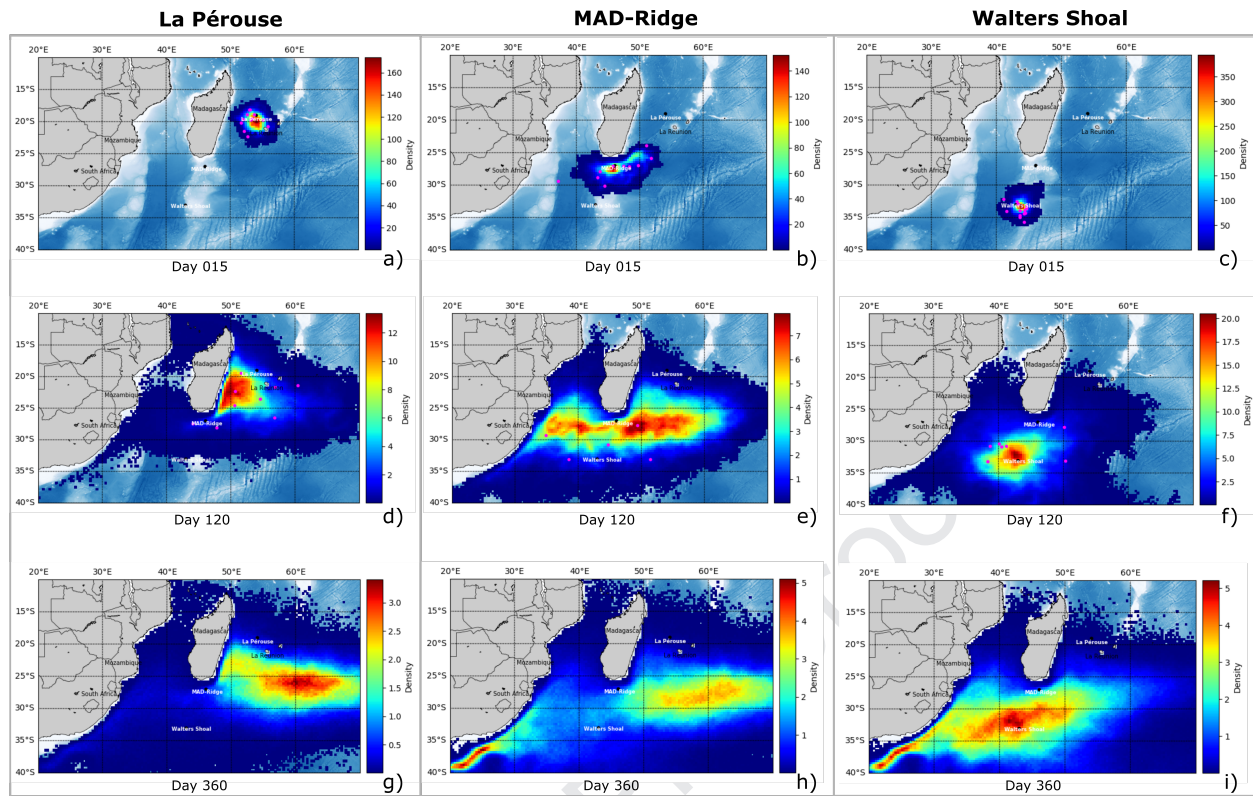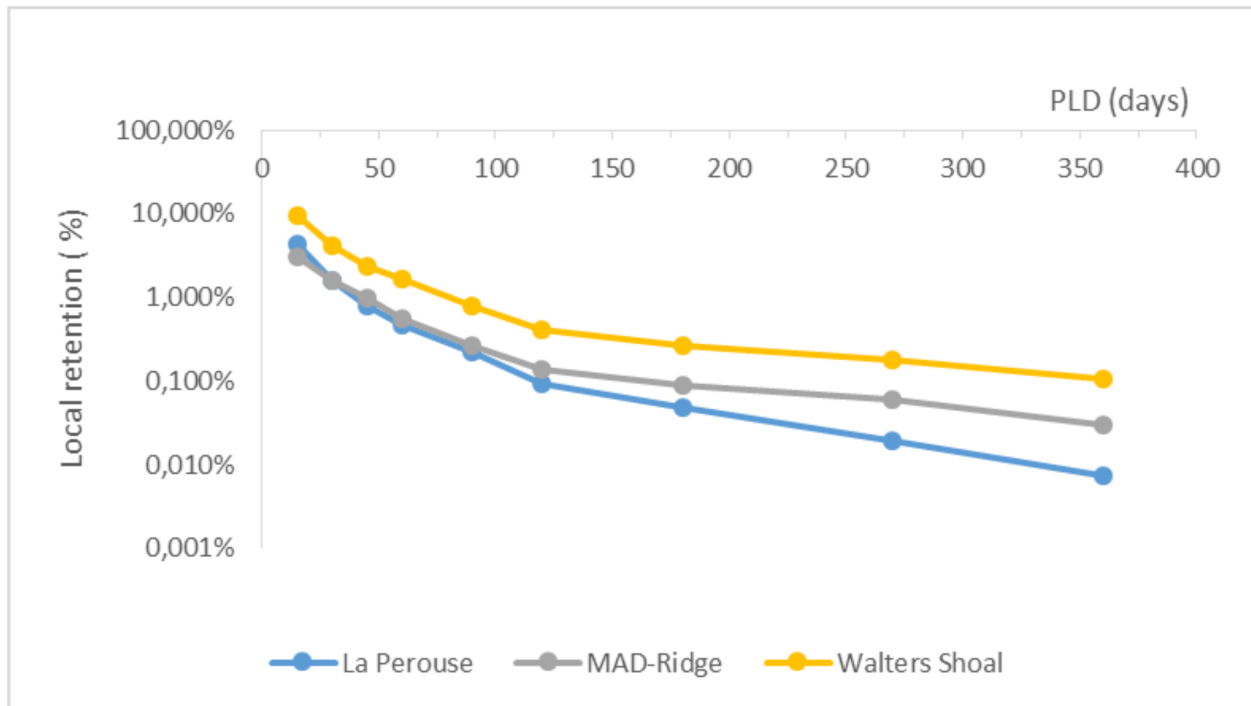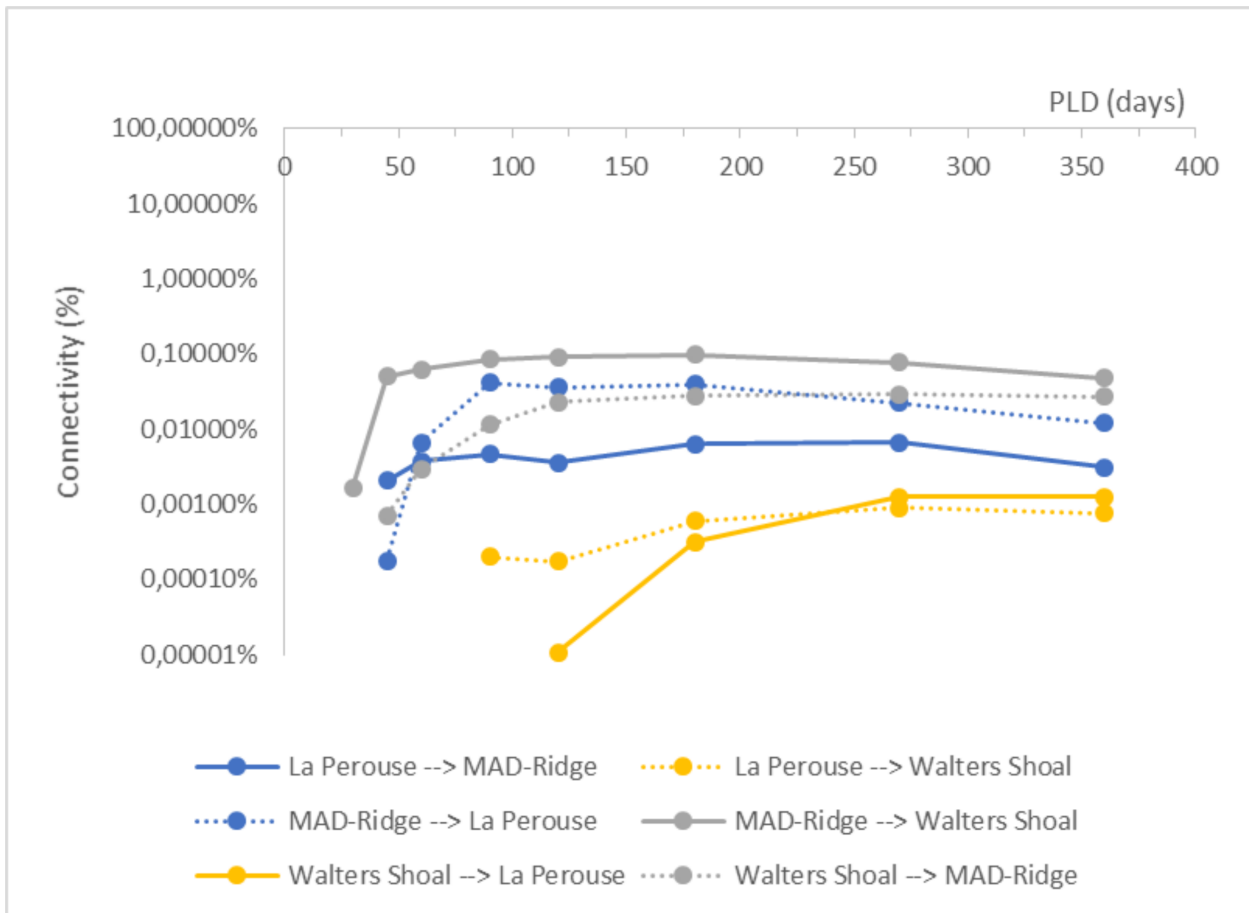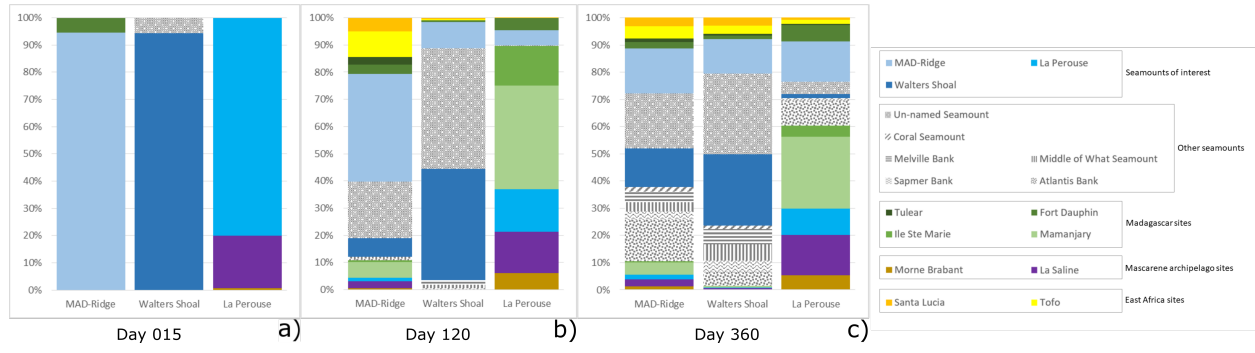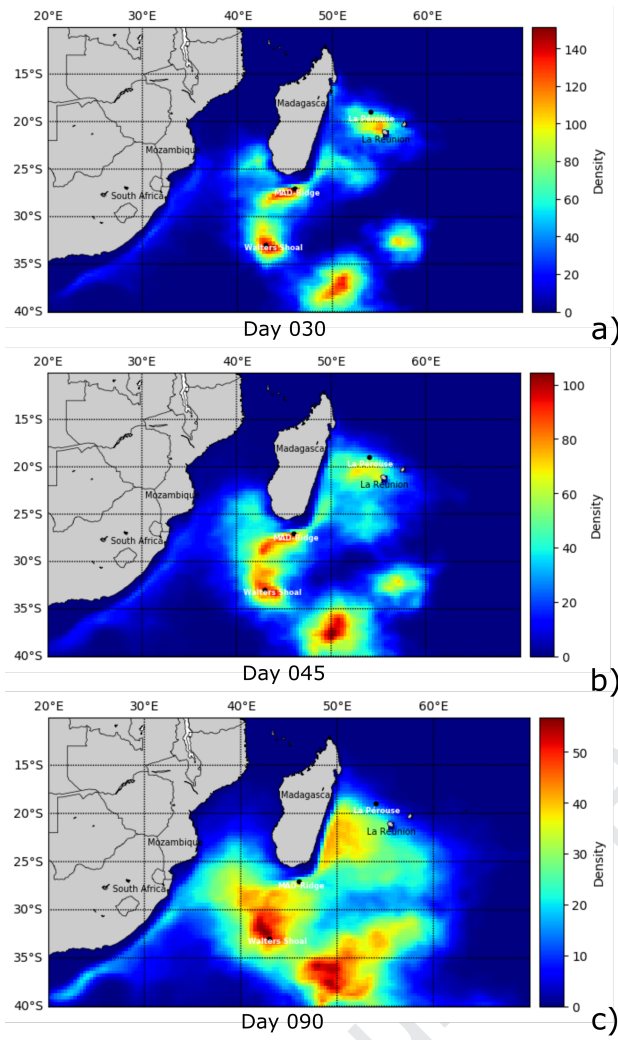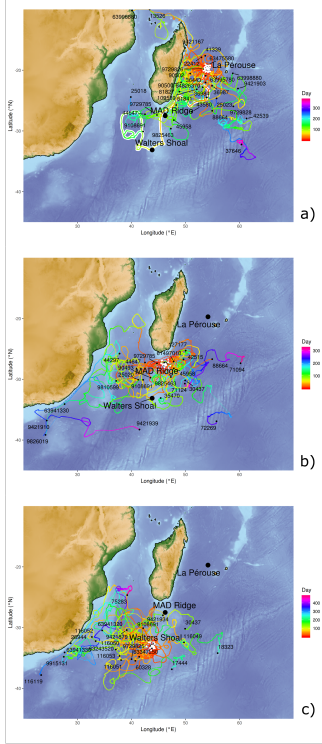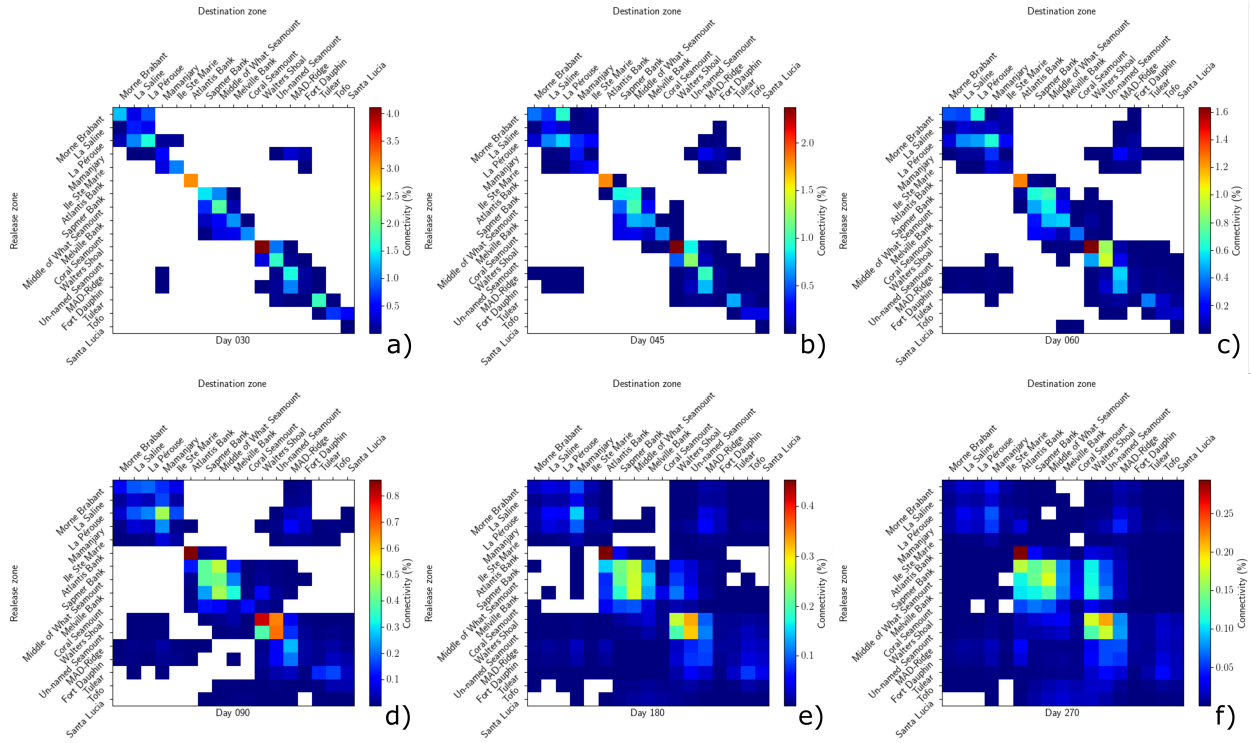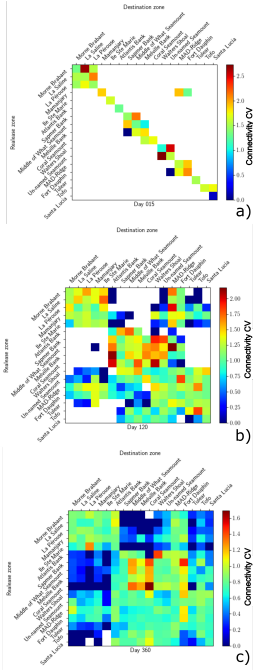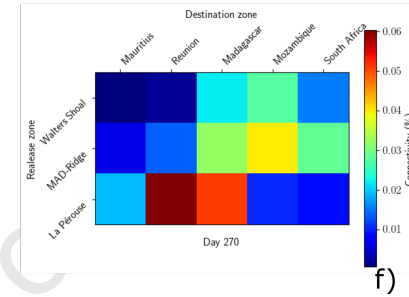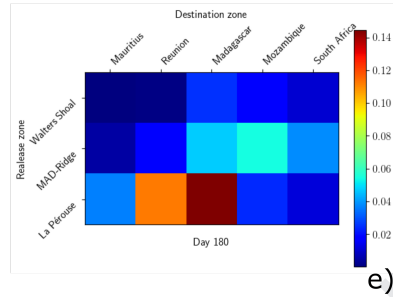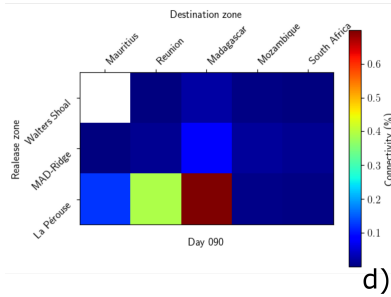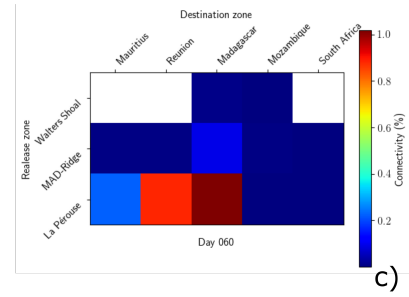
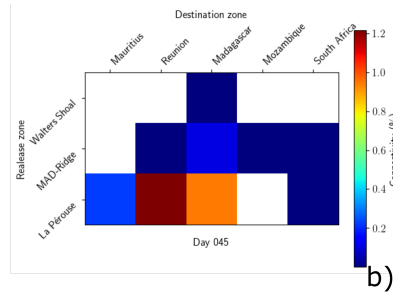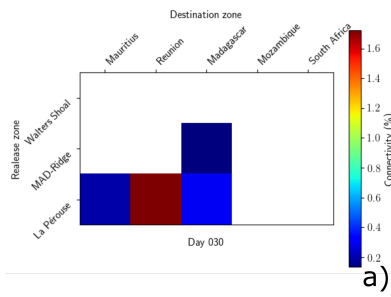**Declaration of interests**

☒ The authors declare that they have no known competing financial interests or personal relationships that could have appeared to influence the work reported in this paper.

☐The authors declare the following financial interests/personal relationships which may be considered as potential competing interests: